Agricultural and Forest Meteorology 357 (2024) 110197

Contents lists available at ScienceDirect

Agricultural and Forest Meteorology

journal homepage: www.elsevier.com/locate/agrformet

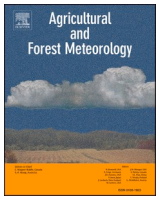

Effects of slow temperature acclimation of photosynthesis on gross primary production estimation

Jia Bai [a,b], Helin Zhang [c], Rui Sun [a,b,*], Yuhao Pan [d]

[a] State Key Laboratory of Remote Sensing Science, Faculty of Geographical Science, Beijing Normal University, Beijing 100875, China
[b] Beijing Engineering Research Center for Global Land Remote Sensing Products, Faculty of Geographical Science, Beijing Normal University, Beijing 100875, China
[c] Research Institute of Agriculture and Life Sciences, Seoul National University, Seoul 08826, Republic of Korea
[d] Research Area of Ecology and Biodiversity, School of Biological Sciences, The University of Hong Kong, Pokfulam, Hong Kong 999077, China

ARTICLE INFO

Keywords:
GPP
SIF
Temperature acclimation
State of acclimation

ABSTRACT

The slow temperature acclimation of photosynthesis has been confirmed through early field experiments and studies. However, this effect is difficult to characterize and quantify with some simple and easily accessible indicators. As a result, the impact of slow temperature acclimation of photosynthesis on gross primary production (GPP) estimation has often been overlooked or not integrated into most GPP models. In this study, we used a theorical variable-state of acclimation (S), to characterize the slow temperature acclimation. This variable represents the temperature to which the photosynthetic machinery adapts and is defined as a function of air temperature (T_a) and time constant (τ) required for vegetation to respond to temperature, to discuss its impact on GPP simulation. We used FLUXNET2015 dataset to calculate S and established a GPP model using S and shortwave radiation (SW) based on random forest algorithm (S model). As a comparison, we directly used T_a and SW to build the other GPP model (T_a model). Moreover, the divergent temperature acclimation capacities of plants are crucial to predict and make preparations for likely temperature stress in the future. Therefore, the spatial distribution of τ values was also mapped using satellite sun induced chlorophyll fluorescence (SIF) and T_a datasets. The results indicated that: (1) taking into account the slow temperature acclimation of photosynthesis led to a more precise estimation of GPP which mainly reflected in reduction of excessive fluctuations in GPP predictions; (2) considering the slow temperature acclimation of photosynthesis can reduce the sensitivity of vegetation to temperature; (3) the improvement of S model in GPP estimations was different in different vegetation growth stages which was more significant in the springtime recovery stage; (4) τ values had significant spatial distribution which was strongly affected by the determinants of vegetation growth and seasonal variations in temperature.

1. Introduction

As a crucial element of terrestrial ecosystems, vegetation assimilates carbon dioxide into carbohydrate and releases oxygen through photosynthesis which drives the global carbon cycle (Anav et al., 2015; Battin et al. 2009; Janssens et al. 2003; Porcar-Castell et al. 2014; Zhang et al. 2022). A key indicator of vegetation photosynthesis, gross primary production (GPP), refers to the total carbon absorbed by vegetation through photosynthesis and holds significant importance in evaluating vegetation functions and quantifying the carbon cycle at various scales (Ma et al. 2015; Zhang et al. 2021). Therefore, quantitative information about GPP is crucial for predictions of photosynthesis and regional or global carbon flux (Beer et al. 2010; Chen et al. 2021a; Chen et al. 2021b; Luo and Keenan 2020; Piao et al. 2020).

Developed GPP models are the principal tools to quantify GPP at different spatio-temporal scales (Badgley et al. 2019; Chen et al. 1999; Cheng et al. 2014; Jiang and Ryu 2016; Jung et al. 2011; Potter et al. 1993; Running et al. 2004; Zhang et al. 2023b). A lot of models integrated the dependence of GPP on various environmental drivers in which temperature is one of the key drivers in the seasonality of GPP (Dusenge et al. 2019; Hikosaka et al. 2006; Kolari et al. 2007; Kumarathunge et al. 2019; Mäkelä et al. 2004). For example, the light use efficiency (LUE) models calculated the temperature stress factor based on air temperature, vegetation optimal temperature, minimum

* Corresponding author at: State Key Laboratory of Remote Sensing Science, Faculty of Geographical Science, Beijing Normal University, Beijing 100875, China.
E-mail address: sunrui@bnu.edu.cn (R. Sun).

https://doi.org/10.1016/j.agrformet.2024.110197
Received 12 October 2023; Received in revised form 12 August 2024; Accepted 15 August 2024

temperature, etc., to characterize the impact of temperature on photosynthesis (Zhang et al. 2023b). In such models, the temperature dependences of vegetation have frequently been directly described by ambient temperature in the form of mathematical models, and vegetation would change its rates of photosynthetic carbon assimilation immediately with temperature changes under these temperature based mathematical models (Lin et al. 2012; Zhang et al. 2023a; Zhang et al. 2023b). However, plants have "memories" for environment, lasting from several minutes to days or even longer, which means that the physiologically response of vegetation to changes in growth temperature is time dependent (Crous et al. 2022; Karban 2008; Trewavas 2009). Indeed, early field experiments and studies have shown that the response of photosynthesis to temperature is time delayed rather than instantaneous response (Gea-Izquierdo et al. 2010; Mäkelä et al. 2004; MÄKelÄ et al. 2008; Wu et al. 2015; Zuther et al. 2015). This strategy was called the slow temperature acclimation of photosynthesis, which indicates that the state of vegetation does not immediately synchronize with the ambient temperature, but takes a certain amount of time to adapt to temperature changes slowly (Mäkelä et al. 2004; MÄKelÄ et al. 2008). Therefore, ignoring the time delay in vegetation temperature acclimation may amplify the sensitivity of vegetation to temperature and lead to the bias in GPP estimation (Aspinwall et al. 2016; Lombardozzi et al. 2015). As such, taking the slow temperature acclimation into account in GPP estimation may have a meaningful impact on more accurate quantifications of regional or global GPP (Crous et al. 2022; Dusenge et al. 2020; Lombardozzi et al. 2015; Smith and Dukes 2017).

Although early studies have investigated the slow photosynthetic temperature acclimation and provided the evidence of its existence (Fang et al. 2023; Gea-Izquierdo et al. 2010; MÄKelÄ et al. 2008; Smith and Dukes 2013; Smith et al. 2016; Wu et al. 2015), as of yet, few studies incorporated this temperature response strategy into GPP models and explored the differences in GPP estimates with and without coupling slow temperature acclimation especially for some empirical, semi-empirical and data driven models (Atkin et al. 2008; Guan et al. 2021; He et al. 2013; Kumarathunge et al. 2019; Wang et al. 2015; Zhang et al. 2023b; Zhang et al. 2011; Zheng et al. 2020). One of the difficulties in incorporating slow temperature acclimation of photosynthesis into GPP models is that it is difficult to accurately characterize and quantify this temperature acclimation strategy through some simple and easily accessible indicators. Mäkelä et al. (2004) developed a theorical variable, state of acclimation (S), to describe the slow temperature acclimation of photosynthesis, which can be considered the temperature to which the photosynthetic machinery adapts and expressed as the following equation (Mäkelä et al. 2004):

$$\frac{dS}{dt} = \frac{T_a - S}{\tau} \tag{1}$$

where T_a is air temperature, S is the state of acclimation, τ is the time constant which represents the time required for vegetation to adapt to air temperature (Mäkelä et al. 2004). S describes the slow temperature acclimation of vegetation in a simple method and also can be easily obtained (Gea-Izquierdo et al. 2010; Kolari et al. 2009; MÄKelÄ et al. 2008).

It is worth noting that Eq. (1) could not only characterize the slow temperature acclimation of photosynthesis, but can be used to evaluate the capacity of vegetation in temperature acclimation to some extent, which is essential in predicting and making preparations for likely temperature stress in the future. For example, the lower τ values in Eq. (1) reflect the faster temperature response of vegetation and stronger temperature acclimation ability, in contrast, the higher τ values indicate slower temperature response of vegetation and less temperature acclimation capacity. The capacities of vegetation to adjust to temperature are always related to the environments which the foliage is exposed. Therefore, vegetation from different environment holds divergent capacities to adjust to temperature which would lead to the spatial differences in the τ values (Cunningham and Read 2003a; Gea-Izquierdo et al. 2010; Kumarathunge et al. 2019; Valladares et al. 2014; Zhang et al. 2023a). However, the uneven and limited distribution of flux sites makes it impossible to get the continuous spatial patterns of τ values at regional or global scales with a flux network, alone (Badgley et al. 2019; Baldocchi 2014; Baldocchi 2003). By comparison, the satellite observations offer an effective mean to continuously assess τ values at larger scales (Frankenberg et al. 2011; Xiao et al. 2019; Zhou et al. 2001). Over the last decades, sun-induced chlorophyll fluorescence (SIF) emitted by terrestrial vegetation has been captured through optical remote sensing (Frankenberg and Berry 2018; Frankenberg et al. 2011; Guanter et al. 2007; Guanter et al. 2012; Mohammed et al. 2019; Zhang et al. 2016). The physiological information included in SIF has great potential and advantages in assessment of vegetation functions (Frankenberg and Berry 2018; Köhler et al. 2018; Krämer et al. 2021; Mohammed et al. 2019; Porcar-Castell et al. 2021; Zhang et al. 2021), which can be used as a fantastic index to analyze the spatial patterns of τ values.

Given the importance of the slow temperature acclimation of photosynthesis in GPP estimation and climate response predictions, this study first simulated GPP with and without considering the slow temperature acclimation using data from flux sites. We then mapped the global spatial distribution of τ values based on satellite SIF datasets. We aimed to investigate the impact of slow temperature acclimation of photosynthesis on GPP prediction and analyze the global spatial patterns of τ values. Our results will meaningfully influence the simulations of GPP, and will be also beneficial for predicting the responses and behaviors of vegetation under global warming.

2. Methodology

2.1. Data

2.1.1. FLUXNET2015

The FLUXNET2015 dataset consists of net ecosystem exchange (NEE) of CO_2 and other meteorological variables from more than 200 sites globally (Pastorello et al. 2020) (https://fluxnet.fluxdata.org/data/). Through flux partitioning, NEE is partitioned into GPP and ecosystem respiration (R_{eco}) (Pastorello et al. 2020). In this study, we collected a total of 212 flux sites from FLUXNET2015 and selected variables including daily GPP based on nighttime flux partitioning method, air temperature and incident shortwave radiance (SW) to investigate the influence of slow temperature acclimation of photosynthesis on GPP estimations. To ensure the quality of the flux data, we checked the seasonal variations of each variable year by year for each flux site and see if there are −9999 values (missing data values are indicated with −9999). Once we found a −9999, we eliminated the data for the whole year where the −9999is located. Then we used the data points without −9999 to calculate S. Finally, we chose high-quality data as determined by the quality flags (quality flag > 0.8) for each variable which is a fraction between 0 and 1 in the daily datasets, indicating percentage of measured and good quality gap filled data, and eliminated the negative GPP values to build and validate the models. After checking the quality, a total of 402,770 flux data points were eventually obtained.

2.1.2. Satellite SIF dataset

We employed satellite SIF as the proxy for photosynthesis to explore the global spatial distribution of τ values. So far, numerous satellite SIF datasets have been generated, which provide an opportunity for large-scale monitoring of terrestrial photosynthesis (Frankenberg et al. 2011; Frankenberg et al. 2014; Porcar-Castell et al. 2014; Sun et al. 2018; Zhang et al. 2016; Zhang et al. 2019). However, the coarse spatial resolution, discontinuous spatial sampling and short-term record of the existing satellite SIF datasets render them inadequate for continuous and long-term analyses (Guo et al. 2020; Hu et al. 2021; Köehler et al. 2018; Yu et al. 2019; Zarco-Tejada et al. 2003). Given that, Zhang et al. (2018) regenerated a global continuous SIF (CSIF) dataset using

satellite-retrieved SIF from the Orbiting Carbon Observatory-2 (OCO-2) and moderate-resolution imaging spectroradiometer (MODIS) surface reflectance based on neural networks, which has higher spatio-temporal resolution (0.05°, 4-day). Therefore, in this study, we selected the all-sky daily average CSIF dataset with 0.05° and 4-day spatio-temporal resolution from 2001 to 2018 to map the global spatial patterns of τ values. We upscaled the spatial resolution from 0.05° to 0.25° based on pixel aggregate method to make its spatial resolution consistent with the ERA-5 dataset.

2.1.3. ERA-5 dataset

In this study, the spatial patterns of τ values were mapped by combining the CSIF dataset with ERA-5, the fifth-generation global land surface reanalysis dataset of the European centre for Medium Range Weather Forecasts (ECMWF), available at a resolution of 0.25° (http://data.ecmwf.int/data). The hourly ERA-5 meteorological variables were downloaded including 2 m air temperature (T_a, °C), 2 m dewpoint temperature (T_d, °C), and downward shortwave radiation (SW, W/m^2) from 2001 to 2018. Then we calculated the daily average 2 m air temperature, average 2 m dewpoint temperature, and total downward shortwave radiation (SW, W/m^2). Lastly, we used T_a and T_d to calculate vapor pressure deficit (VPD, h Pa).

$$SVP = 6.112 \times e^{\frac{17.67T_a}{T_a+243.5}} \tag{2}$$

$$RH = e^{\frac{17.625T_d}{T_d+243.04} - \frac{17.625T_a}{T_a+243.04}} \tag{3}$$

$$VPD = SVP \times (1 - RH) \tag{4}$$

where SVP is the saturated vapor pressure (h Pa) and RH is the relative humidity (Zheng et al. 2020).

2.2. Methods

2.2.1. The calculation of state of acclimation (S)

The state of acclimation, S, developed by Mäkelä et al. (2004) was used to characterize the slow temperature acclimation of photosynthesis which can be expressed in temperature units. Based on Eq. (1), dS can be defined as the function of T_a and time constant τ (days). S time series can be calculated as the following expression based on Eq. (1) (Mäkelä et al. 2004; MÄKelÄ et al. 2008):

$$S_n = S_{n-1} + dS = S_{n-1} + \frac{T_n - S_{n-1}}{\tau},\ S_0 = T_0 \tag{5}$$

where S_n (°C) is the mean daily S on nth day, τ (days) is the time constant, T_n is the mean daily air temperature on nth day, S_0 is the initial value of S. Here, we set S_0 of each site equal to T_a at the beginning of the year.

In this study, we used S (°C) and T_a to simulate GPP, respectively, to compare the differences of GPP estimates with and without coupling the slow temperature acclimation. Based on Eqs. (1) and (5), calculating S involves two parameters: S_0 and time constant, τ. For the S_0, we set S_0 equal to T_a at the beginning of the year in each site. Similarly, we also set S_0 as the average of T_a during the first 10 and 20 days at the beginning of the year, respectively, to test the influence of different initial values of S_0 on the GPP estimation. For the τ values, we first calculated several groups of S time series for different τ values using the daily T_a time series data based on Eq. (5) for each site. Here, we set τ to vary from 1 to 80. Then, for each site, we used each group of S data calculated for different values of τ along with corresponding SW data to predict GPP based on random forest (RF) algorithm, respectively, and evaluated the accuracy of S based GPP estimation for each group of S. Finally, the τ value corresponding to the highest accuracy of the GPP simulation was considered as the optimal time it takes for vegetation to acclimate to temperature. Given the presence of some noise in the changes of R^2 values with increasing values, we initially employed the LOESS (Locally Weighted Scatterplot Smoothing) method to fit the R^2 curve, which is a non-parametric regression technique utilized for data smoothing. Subsequently, we identified the τ values corresponding to the maximal R^2 values through the fitted curves obtained from the LOESS smoothing process. And S calculated using the determined optimal τ value and S_0 was used as an indicator of slow temperature acclimation of photosynthesis to explore its influence on GPP estimations.

Here, we selected several sites to show the accuracy (R^2 values) of GPP estimations based on S calculated for different τ values (from 1 to 80), to display the determination of τ value. Like Fig. 1 displayed, the R^2 values of GPP estimation increased first until meet the peak value then decreased with increasing τ values, and the τ value maximizing R^2 values was chosen as the optimal τ value to calculate the S time series (red circle point in Fig. 1).

2.2.2. The establishment and evaluation of GPP models

To evaluate the influence of slow temperature acclimation of photosynthesis on GPP estimation, we separately built and validated two different kinds of GPP models: T_a model and S model, based on RF algorithm. In T_a model, we didn't consider the impact of slow temperature acclimation of photosynthesis on GPP estimation. GPP was directly estimated using T_a and SW from the flux data using RF algorithm based on Eq. (6):

$$GPP = f(T_a,\ SW) \tag{6}$$

In S model, the slow temperature acclimation of photosynthesis was considered. We used the S calculated in Section 2.2.1 and SW to estimate GPP based on RF algorithm, like the following equation:

$$GPP = f(S,\ SW) \tag{7}$$

We established and validated T_a and S models for each site, respectively. All data points in each site were randomly split into 70% for training and 30% for validation. The coefficient of determination (R^2), root-mean-square error (RMSE) and slope value of regression line (slope) were utilized to assess the accuracy of GPP estimation in comparison to site-observed GPP obtained through the eddy covariance technique (GPP_EC). Meanwhile, in order to compare the contribution differences between T_a and S in GPP estimates, we calculated the importance of T_a and S to GPP estimation based on RF for each site. We also applied Shapley Additive exPlanations (SHAP) value to explain how RF models (S and T_a models) we built to predict GPP time series data, which can reflect the impact of each explanatory variable on GPP predictions, so as to explore the difference between the impact of T_a and S on GPP prediction.

In addition, to investigate the impact of slow temperature acclimation on GPP estimation under different vegetation growth stages, we split the vegetation growth periods into three stages including spring-time recovery of photosynthesis, autumn decline of photosynthesis and rapid growing stage based on *in-situ* GPP observations (Piao et al. 2019). Since there is no photosynthesis in the dormant season for most plants, we didn't analyze the impact of slow temperature acclimation on GPP estimation during the dormant season. For each site, we first smoothed the original *in-situ* GPP_EC time series data to reduce the interference of noisy data based on Savitzky–Golay (SG) filter (Guo et al. 2017). Then we used a double logistic functions of time (day of year, DOY) to fit the smoothed GPP_EC data and detected these three key transition dates through finding the local minimal or maximal rate of change in the curvature of the fitted logistic models (Zhang et al. 2003). There are three local maximum and minimum points, respectively, in the curvature of the fitted logistic model. The key transition dates of the spring-time recovery of photosynthesis correspond to the first 2 local maximal points of the curvature, the key transition dates of the autumn decline of photosynthesis corresponds to the last 2 local minimal points of the curvature and the growing stage corresponds to the second local maximal and second local minimal points of the curvature of the fitted

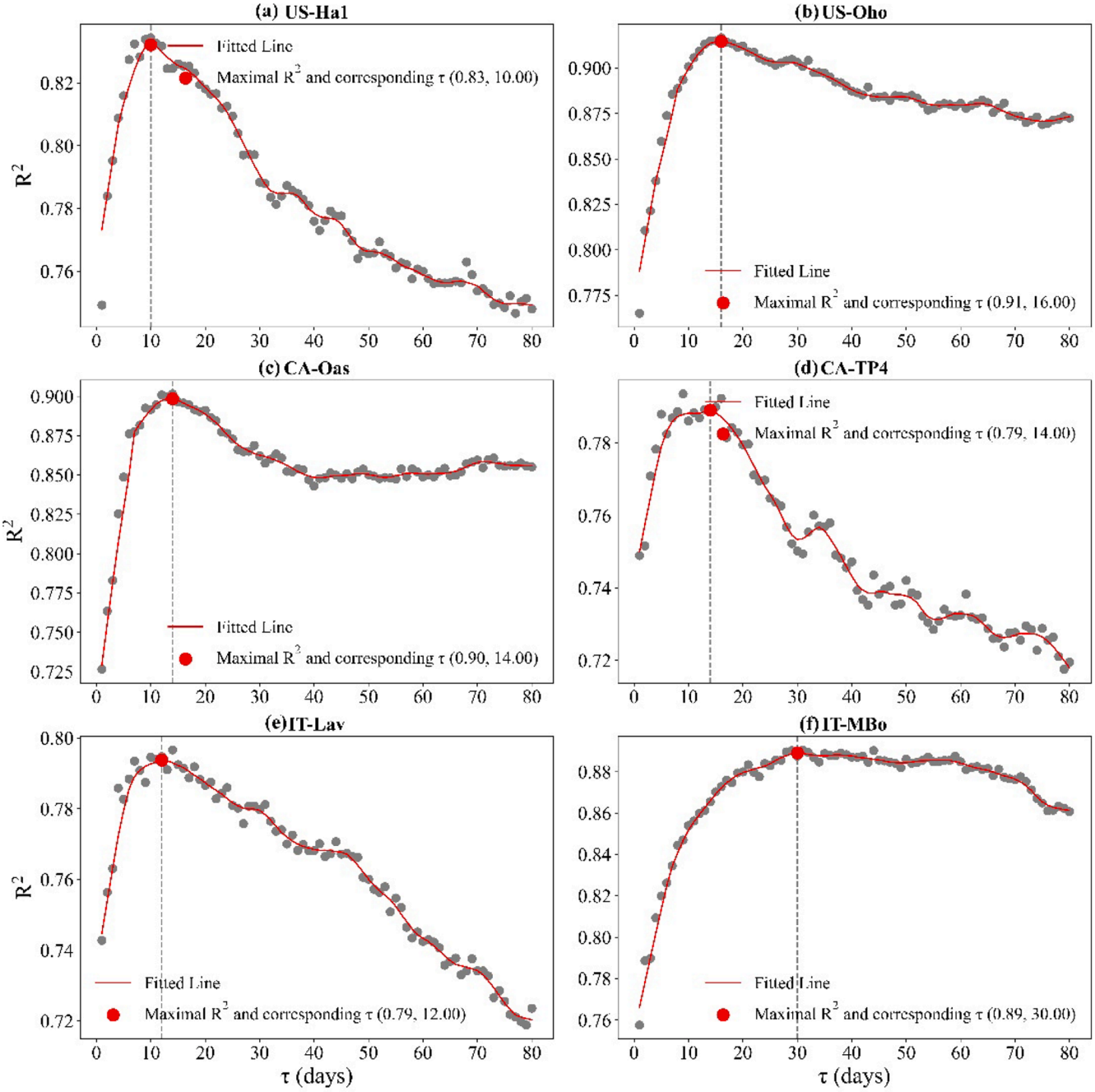

Fig. 1. The R^2 values of GPP estimation based on several groups of S calculated for different τ values (from 1 to 80). The red solid line is the fitted line, the red circle and dashed gray line are the maximal R^2 and corresponding τ value, respectively, and the gray circle is the R^2 values of GPP estimation based on several groups of S calculated for different τ values. (a) is site US-Ha1, (b) is site US-Oho, (c) is site CA-Oas, (d) is site CA-TP4, (e) is site IT-Lav, (f) is site IT-Mbo.

logistic models. Finally, the detected three key transition dates were used to split the validation data.

2.2.3. *The global spatial distribution of τ*

The determination of global τ values was similar to Section 2.2.1. The difference is that the τ values corresponding to the highest correlation between CSIF and S calculated for different τ values was considered as the optimal time it takes for vegetation to acclimate to temperature for each pixel. We used ERA-5 T_a data from 2001 to 2018 to calculate the global long-term S time series data for several τ values based on Eq. (5). S_0 was set as the initial T_a value in 2001 for each pixel and τ was set to vary from 1 to 20. Since the temporal resolution of CSIF is 4-day, the values of τ we set actually corresponded from 4 to 80 days. For each pixel, we separately calculated the correlation between each group of S calculated for different τ values and CSIF from 2001 to 2018, and chose the corresponding τ value with the highest correlation between S and CSIF as the optimal temperature response time. In order to analyze the spatial patterns of τ values, we also calculated the importance of T_a, SW and VPD to CSIF from 2001 to 2018 based on RF. Moreover, we calculated the global importance of S and T_a to CSIF and compared the spatial difference between their importance.

3. Results

3.1. The influence of slow temperature acclimation on GPP estimation

The influence of various S_0 on the GPP estimation was depicted in Figs. S1 and S2. Importantly, regardless of the specific value chosen for S_0, small differences were observed among S based GPP estimations. Consequently, our focus in the subsequent sections is primarily on the results obtained when S_0 was set to T_0. Fig. 2 showed the performance of GPP estimations based on T_a (Fig. 2a) and S models (Fig. 2b), respectively. For T_a model, the R^2, RMSE and slope values were 0.62, 2.59 g C/m^2/d and 0.69, respectively. For S model, the R^2, RMSE and slope values were 0.74, 2.17 g C/m^2/d and 0.78, respectively. Compared to T_a model, the R^2 and slope values of S model were increased 19.35% and 13.04%, respectively, and the RMSE value was reduced 16.21%. In terms of R^2, RMSE and slope values, S model performed better than T_a model which indicated that considering the slow temperature acclimation of photosynthesis could improve the accuracy of GPP estimation. The performance of T_a and S models in different vegetation types was summarized in Fig. 3. For each vegetation type, the R^2 and slope values of S model were both higher than those of T_a model, the RMSE value of S model was lower than that of T_a model. Among different vegetation types, the improvement of GPP estimation based on S model in EBF was not as significant as in other vegetation types ($R^2_{S\ model}$=0.67, $R^2_{Ta\ model}$=0.64; RMSE $_{S\ model}$=2.4 g C/m^2/d, RMSE $_{Ta\ model}$=2.5 g C/m^2/d; slope $_{S\ model}$=0.71, slope $_{Ta\ model}$=0.69).

Fig. 4 exhibited the comparison of GPP estimates based on S model and T_a model in springtime recovery stage of photosynthesis (Fig. 4a, 4b), decline of autumn (Fig. 4c, 4d) and rapid growing season (Fig. 4e, 4f), respectively. Compared to T_a model, the R^2 value of S model in the spring recovery of photosynthesis improved from 0.48 to 0.63, the RMSE value of S model reduced from 2.53 to 2.07 g C/m^2/d, and the slope value of S model increased from 0.69 to 0.78 (Fig. 4a-b). The validation of S model (Fig. 4c) and T_a model (Fig. 4d) in autumn decline stage of photosynthesis showed that the R^2, RMSE and slope values of T_a model were 0.63, 2.07 g C/m^2/d and 0.78, respectively. The R^2, RMSE and slope values of S model were 0.70, 1.86 g C/m^2/d and 0.82, respectively. Although S model performed better than T_a model in both springtime recovery and autumn decline stage of photosynthesis, the improvement of GPP estimation based on S model in autumn decline stage was lower than that in springtime recovery stage. In springtime recovery stage, the R^2 value of S model improved 31.25%, the RMSE value of S model reduced 18.18% and slope value of S model increased 13.04%. While in autumn decline stage, R^2 value of S model improved 11.11%, the RMSE value of S model reduced 10.14% and the slope value of S model increased 5.13%. Additionally, both T_a and S models in autumn decline stage performed better than in springtime recovery stage, possibly due to the unaccounted complexity of photosynthesis recovery in spring within our model. As shown in Fig. 4e, 4f, during the rapid growing season, the accuracy of S based GPP estimation (Fig. 4e) was higher than that of T_a based GPP estimation (Fig. 4f). The R^2 value of S model improved 15.09%, the RMSE value of S model reduced 13.10% and the slope value of S model increased 12.90%.

In each vegetation growth stage, the scatter plot of GPP estimations based on T_a model was more discrete than that of GPP estimations based on S model. The growth stage with significant differences in scatter plot dispersion between S and T_a models was in the springtime recovery stage of photosynthesis.

3.2. Difference between the impact of T_a and state of acclimation (S) on GPP estimation

In order to analyze what exact influence of slow temperature acclimation of photosynthesis on GPP estimation, we chose several typical flux sites and plotted the seasonal variations of GPP_EC and GPP estimations based on T_a (GPP_T_a) and S (GPP_S) models, respectively (Fig. 5). In general, T_a and S models characterized the overall seasonal patterns of GPP_EC similarly in each selected site which increased first until reach the peak value then declined. Fig. 6 was the scatter plot of the importance of T_a and S to GPP estimations for each site. There was no much difference between the importance of T_a and S which indicated that T_a and S were both important in GPP estimations, and the improvement of the S based GPP estimates was not due to the significant improvement in the importance of state of acclimation (S). GPP_T_a had many fluctuations which deviated excessively from GPP_ EC especially during the springtime recovery stage and the dormant season. There were also fluctuations in GPP_T_a during the autumn decline stage and the rapid growing season, but the performance of GPP_T_a in these two growth stages were better than that in springtime recovery stage and dormant seasons (Fig. 5a). GPP_S effectively avoided the excessive fluctuations which was more consistent with GPP_EC (Fig. 5b). Actually, the fluctuation trend of GPP_T_a and GPP_S were both basically consistent with those of GPP_EC induced by temperature changes. But the fluctuations captured by GPP_T_a seemed a little out of control which was the main difference between GPP_T_a and GPP_S and also the reason for the improvement of GPP estimations based on S model. The slow temperature acclimation of photosynthesis leads to relatively slow and gentle changes in the state of vegetation with ambient temperature changes.

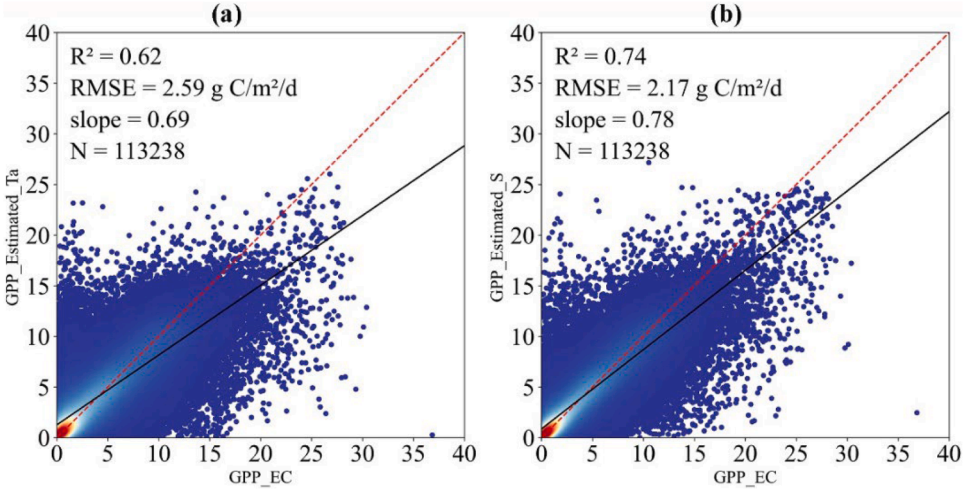

Fig. 2. Comparison of GPP estimates based on (a) T_a model and (b) S model against GPP_EC. GPP_Estimated_Ta is the GPP estimation based on T_a model, GPP_Estimated_S is the GPP estimation based on S model, GPP_EC is site-observed GPP obtained through the eddy covariance technique.

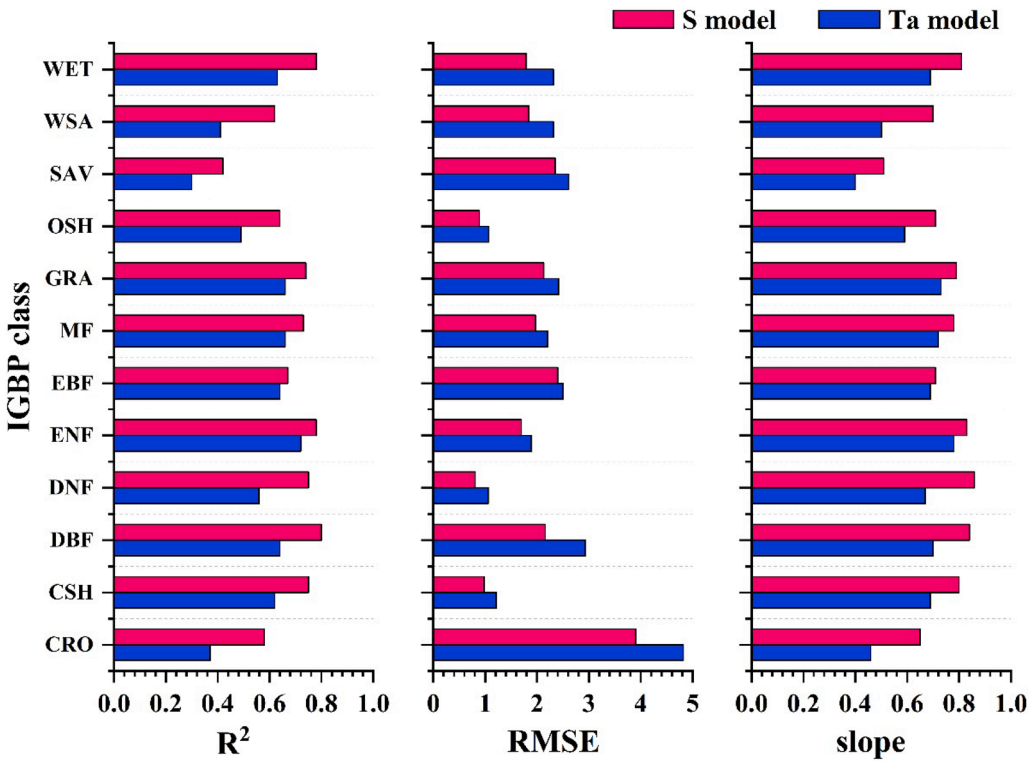

Fig. 3. The performance of GPP estimation based on T_a and S models in each vegetation type. The vegetation types include cropland (CRO), closed shrubland (CSH), deciduous broadleaf forest (DBF), deciduous needleleaf forest (DNF), evergreen needleleaf forest (ENF), evergreen broadleaf forest (EBF), mixed forest (MF), grassland (GRA), open shrubland (OSH), savanna (SAV), woody savanna (WSV) and permanent wetland (WET).

Considering this effect in GPP predictions was more in line with the temperature acclimation strategy of vegetation. On the contrary, without considering the slow temperature acclimation of vegetation, T_a model may amplify the impact of temperature on GPP which may lead to the overreactions of GPP to temperature, and further lead to the uncontrolled fluctuations in GPP_T_a (Fig. 5a).

Fig. 7 was the SHAP values of T_a and S in GPP predictions at the corresponding selected sites in Fig. 5 which could reveal the impact of T_a and S on GPP outputs in T_a and S models. For both T_a and S models, the SHAP values of T_a and S had similar and clear seasonality with bell-shaped curves which indicated that the ability of S and T_a to characterize the seasonality of GPP was similar. In the dormant season, the SHAP values of T_a and S were less than zero, implying that T_a and S were both negatively impact the GPP estimation. Except for the dormant season, the SHAP values of T_a and S were larger than 0 and increased first then decreased, meaning that T_a and S had active impact on GPP estimation and their influence increased first then decreased. The difference between SHAP values of T_a and S was that the fluctuations of T_a SHAP values were more significant and larger than that of S SHAP values especially during the seasonal transitions which was consistent with the difference between S based and T_a based GPP estimations (Fig. 5). To a certain extent, in GPP predictions, considering the slow temperature acclimation of photosynthesis could reduce the sensitivity of GPP to temperature, thereby reducing the errors caused by the excessive fluctuations of GPP estimations induced by changes in temperature when directly using T_a to predict GPP.

In a word, S and T_a both were important in GPP estimation and could capture the overall seasonal patterns of GPP_EC well. However, considering the slow temperature acclimation of photosynthesis could effectively avoid the excessive fluctuations in GPP estimation especially during the seasonal transitions.

3.3. The global spatial distribution of τ values

Fig. 8 showed the global spatial distribution of τ values along with the latitude-based statistical results of τ. The τ values had significant spatial pattern. In high latitude regions (above 30°N) of the Northern Hemisphere, Southeast China, Southern South America, Central and Eastern South America and Central Africa, τ values were lower. In Mexico, India, Southeast Asia, Southern Africa, Australia, and central South America, the τ values were higher. In the high latitude regions (above 30°N) of the Northern Hemisphere, τ values showed a tiny decreasing trend as latitude decreased. In the low latitude regions of the North Hemisphere (0~30°N), τ values increased with decreasing latitude. In the Southern Hemisphere, τ values increased first then decreased with increasing latitude.

Fig. 9 was the spatial distribution of the importance of SW, VPD and T_a to CSIF. In the high latitude of North Hemisphere (above 30°N), T_a and SW had the highest importance which indicated air temperature and radiation were the main determinants for vegetation growth. The regions above 30°N were consistent with regions with lower τ values. In most regions of Mexico, North and Central South America, India, Southeast Asia, most regions of Africa excluding central regions near the equator, and Northern and Eastern Australia, the importance of VPD was much higher than that of T_a and SW which was consistent with regions with higher τ values (except for the Northern and Central Africa).

We calculated the global state of acclimation (S) from 2001 to 2018 based on ERA-5 T_a data and the τ values obtained in Fig. 8, and calculated the importance of S and T_a to CSIF based on RF, respectively. Fig. 10 showed the importance of S (a) and T_a (b) to CSIF, respectively. The spatial distribution of the importance of S and T_a were similar which both exhibited higher importance in the high latitude regions of the Northern Hemisphere (above 60°N), China, Central and Eastern America; in Eastern South America, Central Africa and Central Australia, the importance of S and T_a were both lower; in northern and southern regions of South America, Southern Africa, Southeast Asia, India, and most

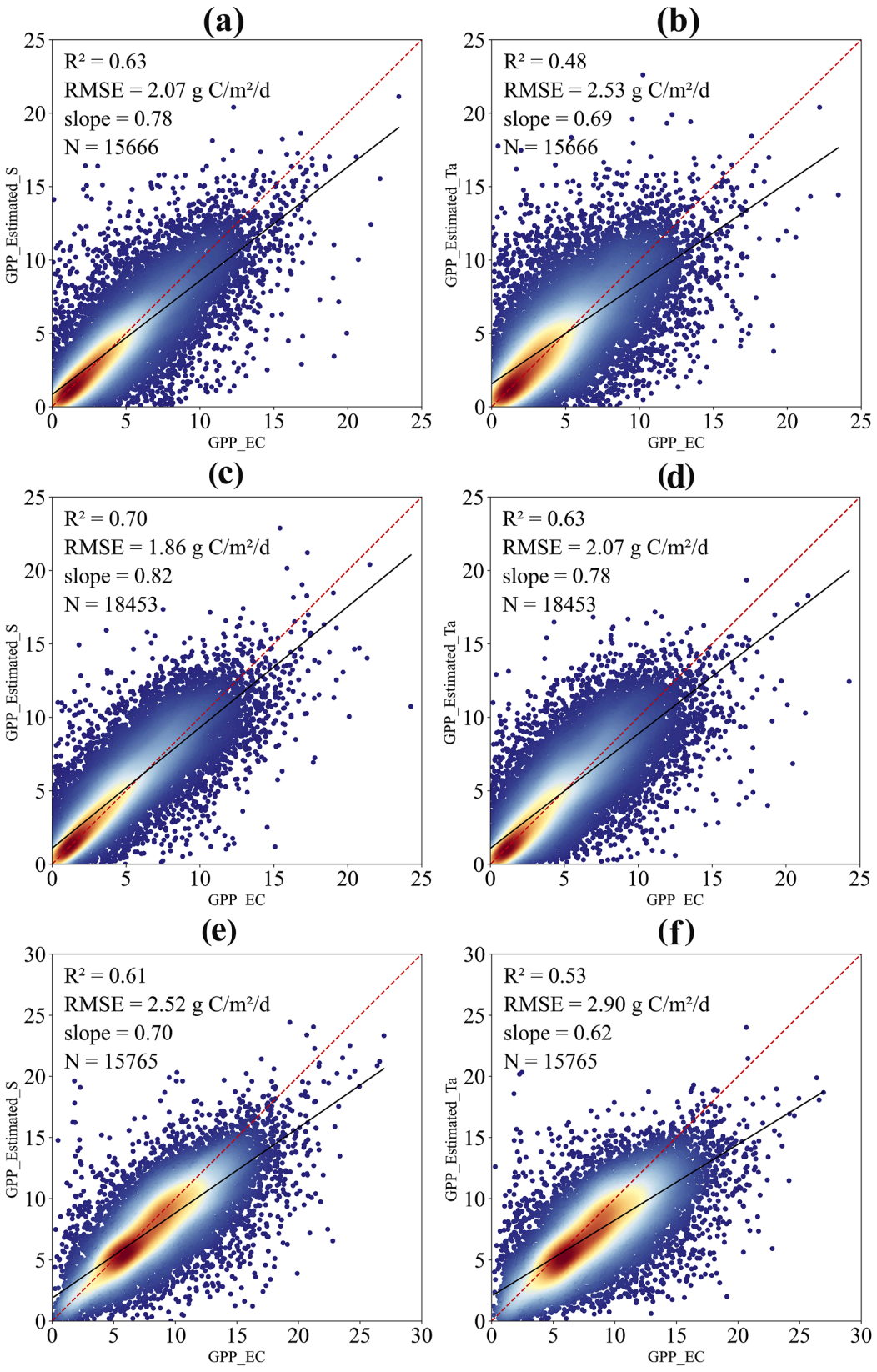

Fig. 4. Comparison of GPP estimation based on S model and T_a model against GPP_EC in springtime recovery stage of photosynthesis (a, b), autumn decline stage of photosynthesis (c, d) and rapid growing season (e, f), respectively. GPP_Estimated_S is the GPP estimation based on S model, GPP_Estimated_Ta is the GPP estimation based on T_a model, GPP_EC is site-observed GPP obtained through the eddy covariance technique.

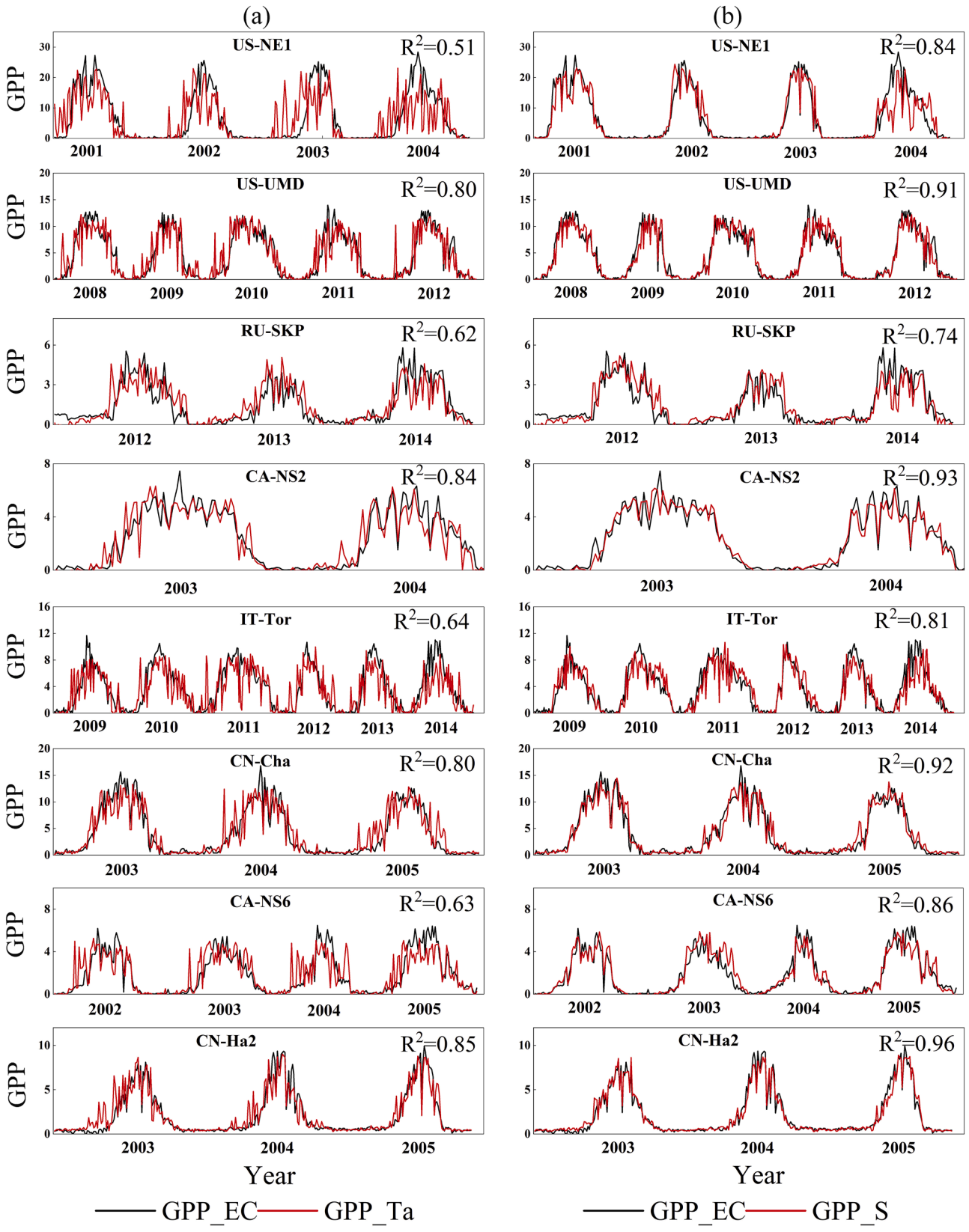

Fig. 5. The seasonal variations of GPP_EC (black dashed line) and GPP estimations based on T_a model (GPP_T_a) (red dashed line in panel a) and S model (GPP_S) (red dashed line in panel b) at several sites (unit: g C/m^2/d).

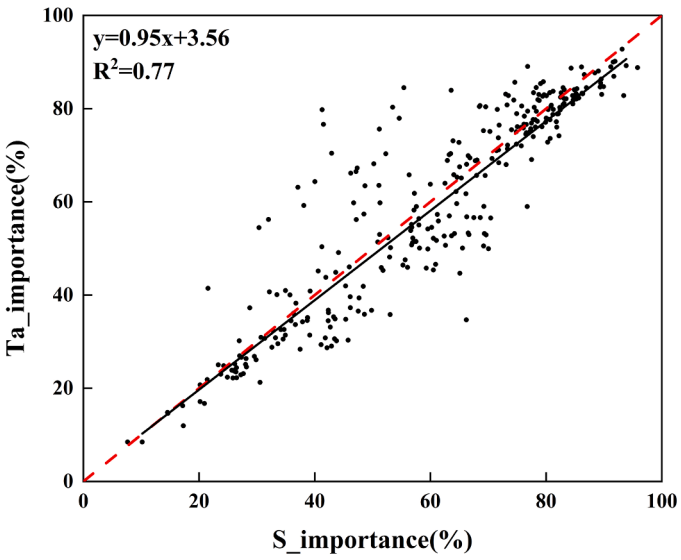

Fig. 6. The importance of S and T_a to GPP estimation for each flux site. The red dashed line is 1:1 line and the black solid line is the regression line.

areas of Australia, the importance of S and T_a were in middle. Fig. 11 displayed the difference between the importance of S and T_a to CSIF. In the most regions of the United States and Canada, Western Europe, Northwest India and Southeast China, southern and northern South America, the difference between importance of S and T_a was less than 0 which indicated that the importance of S was lower than that of T_a. In regions where the difference was less than 0, we may overestimate the importance of temperature to photosynthesis. That is to say, although temperature is the determinant for vegetation growth in these regions, if we do not consider the impact of slow temperature acclimation of photosynthesis, the importance of temperature to vegetation growth may be overestimated and the actual importance of temperature may not be as higher as we previously understood. In Mexico, central South America, Africa, Australia except the central region, Southeast Asia and Southern and Eastern India, the difference between importance of S and T_a was larger than 0 which indicated that the importance of S was higher than that of T_a. The climate in the regions where difference was larger than 0 is warmer and temperature is less important for vegetation growth anymore. However, in these regions, the importance of temperature to vegetation growth may not be as lower as we understood before which may be underestimated if we don't consider the slow temperature acclimation of photosynthesis.

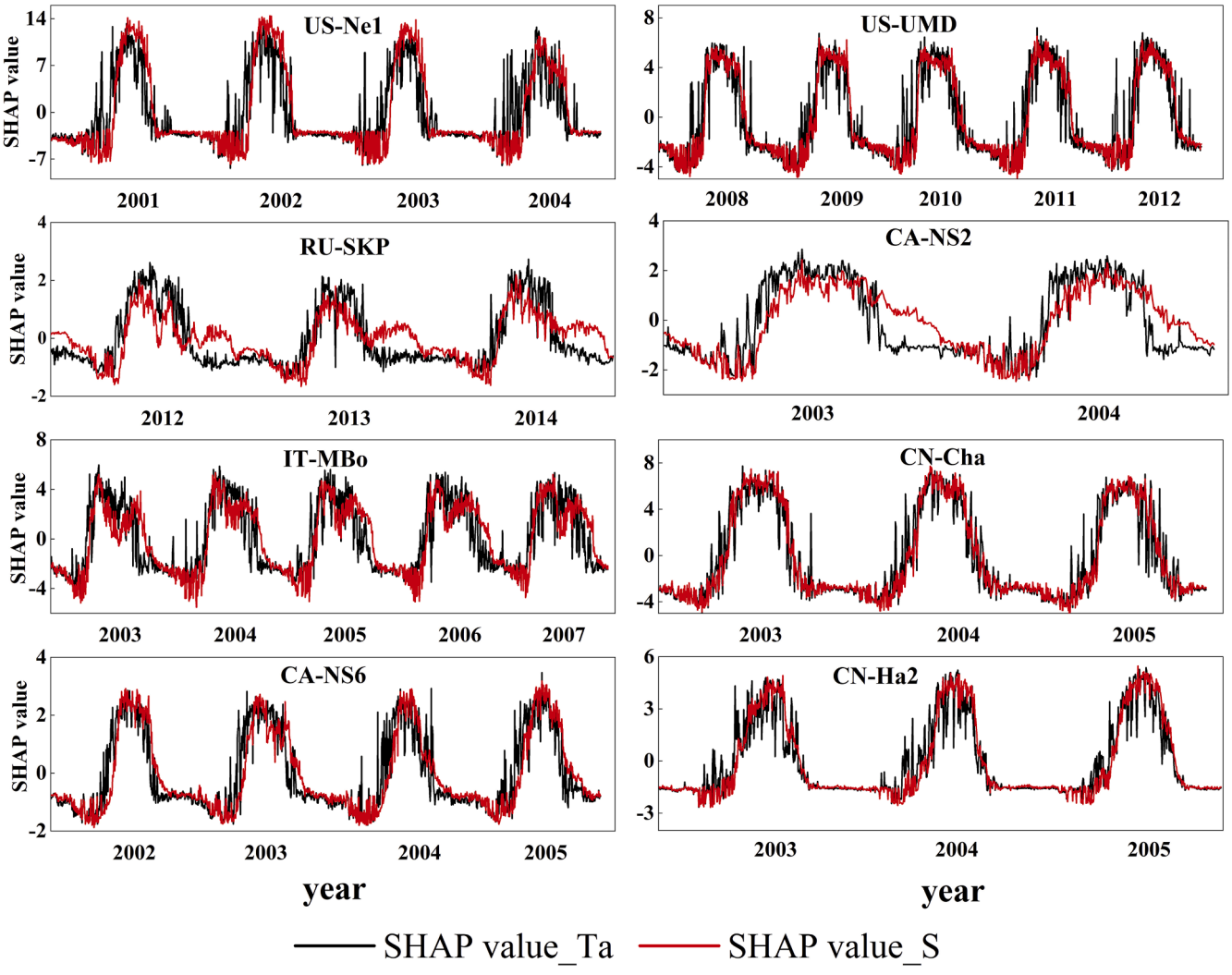

Fig. 7. The SHAP value of T_a and S for several sites. The red solid line is the SHAP value of S, the black solid line is the SHAP value of T_a.

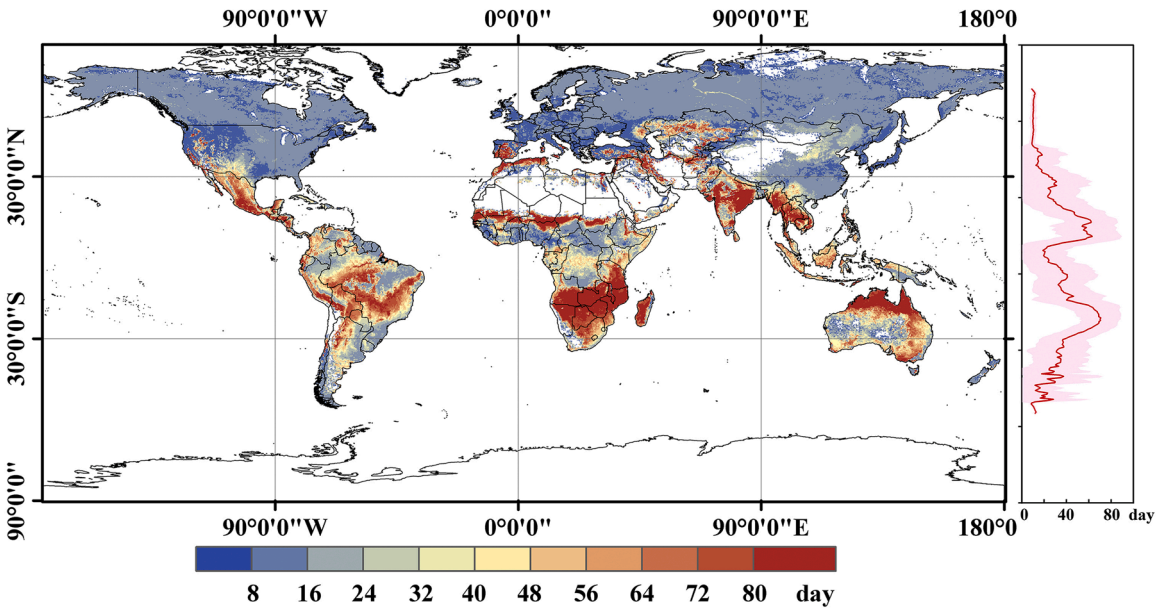

Fig. 8. The spatial distribution of τ values.

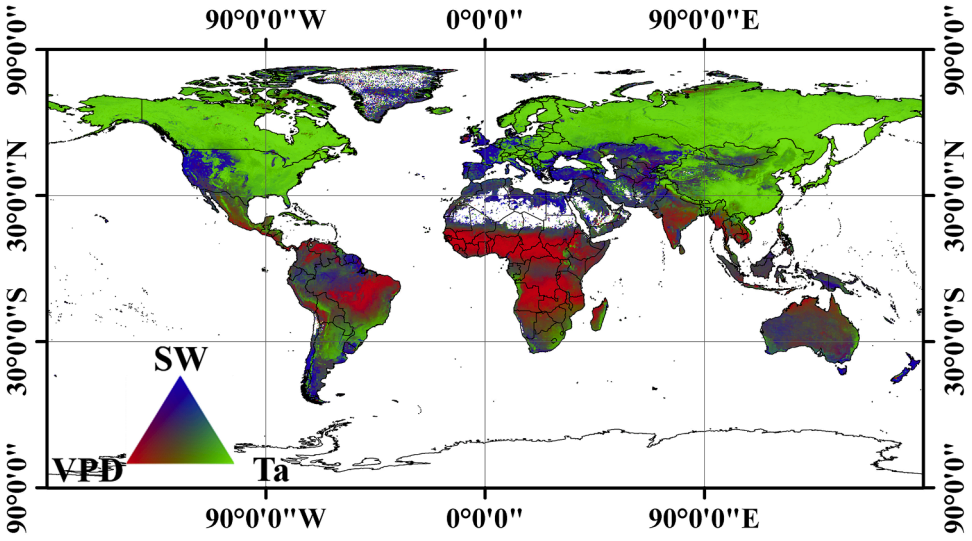

Fig. 9. The spatial distribution of importance of SW, VPD and T_a to CSIF.

4. Discussion

4.1. The influence of slow temperature acclimation of photosynthesis on GPP estimation

Our results showed that considering the slow temperature acclimation of photosynthesis could improve the accuracy of GPP estimation (Fig. 2). This improvement was mainly due to the excessive fluctuations in T_a based GPP estimation, while S based GPP estimation effectively avoided the excessive fluctuations as shown in Fig. 5. When directly using T_a to estimate GPP without considering the slow temperature acclimation of photosynthesis, the sensitivity of vegetation to temperature was amplified, leading to the excessive fluctuations in GPP prediction. The SHAP values of T_a and S can also indicate that the impact of T_a on GPP prediction fluctuated greater than that of S (Fig. 7).

Actually, the time delayed response strategy of vegetation to temperature causes the state of vegetation cannot be synchronized with the ambient temperature changes immediately. Therefore, the temperature state of vegetation directly characterized by T_a cannot represent the true physiologically response of vegetation to changes in growth temperature, which will bring bias in GPP quantification. Like our results shown in Sections 3.1 and 3.2, the T_a model didn't consider the slow temperature acclimation of photosynthesis, and the GPP estimation derived from T_a indeed exhibited some uncontrolled or excessive fluctuations. By comparison, the GPP derived from S model reduced this phenomenon a lot. Moreover, the SHAP values of S and T_a had clear and similar seasonality and their importance in GPP estimation had no much difference which to some extent indicated that there was no much difference in the ability of T_a and S to characterize the overall seasonality of GPP although the S based GPP estimation had better performance than T_a based.

In addition, there were differences in the degree of improvement in S based GPP estimation for different vegetation types and phenology. The improvement of S model in EBF was not as significant as in other vegetation types (S model: R^2=0.67, RMSE =2.4 g C/m^2/d, slope =0.71; T_a model: R^2 =0.64, RMSE =2.5 g C/m^2/d, slope =0.69). The lower

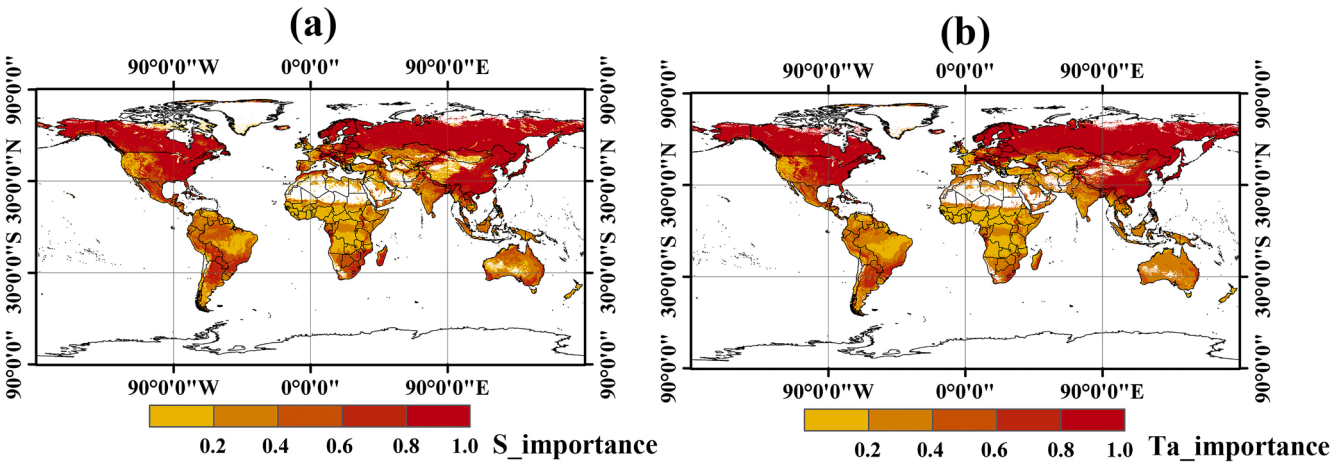

Fig. 10. The global patterns of importance of S (a) and T_a (b) on SIF.

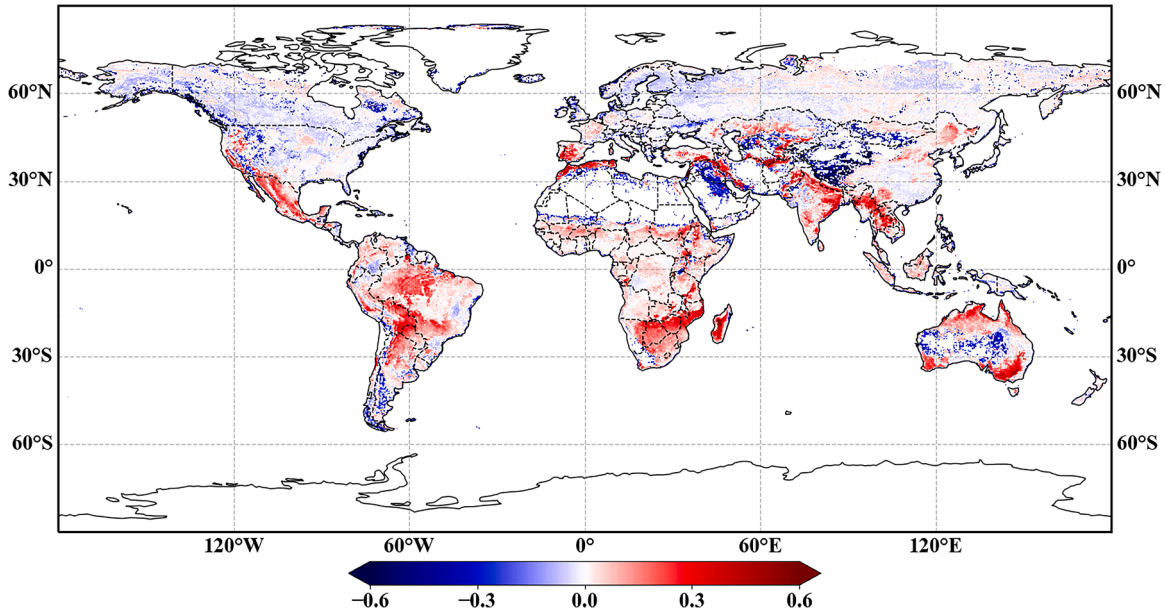

Fig. 11. The spatial distribution of difference between the importance of S and T_a to CSIF.

importance of temperature to vegetation growth could be contributed to the less significant improvement of S model in EBF a lot. Mostly EBF distributed in subtropical and tropical latitudes where temperature is no longer a limiting factor for vegetation growth (Crous et al. 2022). Therefore, for most EBF distributed in warmer regions, considering the slow temperature acclimation of photosynthesis or not had less impact on the GPP estimation. In the springtime recovery stage, growing season and autumn decline stage, the R^2 values of S model were improved 31.25%, 15.09% and 11.11%, respectively; the RMSE values of S model were reduced 18.18%, 13.10% and 10.14%, respectively. The larger improvement in GPP estimation based on S model appeared in the spring recovery stage of photosynthesis, meaning that the influence of slow temperature acclimation of photosynthesis on GPP estimation was relatively higher in this stage (Fig. 4). In the springtime recovery stage of photosynthesis, the plant metabolism has not completely recovered to the non-stress state (Leuendorf et al. 2020; Zuther et al. 2015). Regardless of how the ambient temperature fluctuates, the lower metabolism of plants will make plants insensitive to changes in temperature (Preston and Sandve 2013). Therefore, directly using ambient temperature to predict GPP in the springtime recovery stage will amplify the sensitivity of vegetation to temperature and lead to many excessive fluctuations like the details showed in Fig. 5a. In the rapid growing season and the autumn decline stage, vegetation metabolism is fully restored and the sensitivity of vegetation to temperature is relatively higher, thereby, the synchronization of photosynthesis and temperature is also higher. Hence, the difference between GPP estimation based on S model and T_a model in the rapid growing and autumn decline stages was not as higher as in the springtime recovery stages. That's the reason why the improvement of S model was larger in the springtime recovery stages than that in rapid growing and autumn decline stages. The divergent improvements of S model in different phenology can also reveal that there are seasonal differences in the response ability of vegetation to temperature changes. Therefore, the influence of considering the slow temperature acclimation of photosynthesis on GPP estimation is indeed different in each vegetation phenology like our results showed in Fig. 4.

4.2. The causes and driving factors of global spatial distribution of τ

Previous studies demonstrated that plants in warmer areas have less capacity to adjust to temperature than in cooler regions, leading to the shorter time it takes for vegetation in cooler areas to respond to temperature changes, which was basically consistent with our results

(Carter et al. 2020; Crous et al. 2022; Cunningham and Read 2003a; Cunningham and Read 2003b). As displayed in Fig. 8, the lower τ values were mainly distributed in cooler regions and the higher τ values were distributed in the warmer regions. In order to reduce the negative effects of unfavorable environmental conditions, plants would flexibly adopt different response strategies in the face of different determinants of vegetation growth to adjust the sensitivities of vegetation to environmental conditions synchronously (Kumarathunge et al. 2019; Mkel et al. 2002; Preston and Sandve 2013; Sabot et al. 2022; Trewavas 2009). In regions with lower τ values (except for Central Africa), the determinant of vegetation growth is ambient temperature (Fig. 9). To make sure the plants in temperature limited environmental conditions survive, plants will improve their sensitivities to temperature to capture a sufficient part of the available temperature which was beneficial for vegetation growth especially for the plants distributed in the cooler areas (e.g., the high latitude regions of northern hemisphere). Once temperature rises which is beneficial for vegetation growth, plants would capture the limited suitable temperature to grow as soon as possible, ensuring their survival, which could lead to the shorter time (lower τ value) required for vegetation to respond to temperature changes. Similarly, in order to avoid the negative impact of temperature drop on photosynthesis, vegetation may adjust its state quickly which would lead to shorter response time for vegetation to temperature changes. The regions with higher τ values included Mexico, India, Vietnam, Central South America, southern Africa, Northern and Eastern Australia. The result of importance analysis showed that VPD is the determinant for vegetation growth in these regions rather than temperature which implied that the sensitivity of vegetation to VPD was higher than that of temperature (Fig. 9). Therefore, plants will try their best to respond to changes in VPD as quickly as possible rather than temperature changes since the fluctuations in temperature has less impact on vegetation growth which would lead to longer response time to temperature changes (higher τ values) in these regions. Conversely, the time it takes for vegetation to respond to VPD in these regions may be shorter than in other regions. Because different limiting factors for vegetation growth will lead to different response strategies.

Here, we need to emphasize the complexity of τ values in Africa. In central Africa, the τ values were lower while in Southern Africa, the τ values were higher. However, the result of importance analysis showed that VPD was the determinant for the vegetation growth in both Central and Southern Africa (Fig. 9). The main difference between these two regions is soil moisture, which was higher in Central Africa than that in Southern Africa. The relationship between environmental moisture and temperature acclimation of vegetation is complex and has debates (Dusenge et al. 2020; Hember et al. 2017; Reich et al. 2018). Studies demonstrated that the only warming in wet regions can enhance tree growth (Hember et al. 2017). Did these studies imply that trees might less sensitive to changes in temperature under water limitations? If it does, the vegetation in Southern Africa with lower humidity may be less sensitive to temperature changes, leading to higher τ values. In contrast, the sensitivity of vegetation to temperature in Central Africa is higher and the τ values are relatively lower. Moreover, the quality of OCO-2 SIF data and MODIS reflectance data in the tropical regions is influence by the cloud which may lead to the uncertainties of τ values in Africa. Therefore, in the future study, the exact reason why the spatial distribution of τ values were divergent in Central and Southern Africa need to be explored further.

Additionally, the primary climate shifts from boreal to temperate and tropical regions involve not only rising temperatures but also diminished temperature seasonality, which may be another factor contributing to the observed spatial patterns in τ values (Carter et al. 2020; Cunningham and Read 2003b). It is more likely to respond to temperature changes more quickly for the vegetation exposed to larger seasonal variations in temperature (Berry and Bjorkman 1980). Therefore, vegetation from environments in which the seasonal variations of temperature are larger, shows a greater ability to respond to temperature changes and further leads to lower τ values. In our results, the lower τ values mainly distributed in the boreal or temperate regions in which the temperature seasonal variations are larger. By comparison, the larger τ values mainly distributed in the regions with small seasonal temperature variations like the tropical regions. Overall, the spatial pattern of τ values is likely to be an adaptation to the determinants of photosynthesis and amplitude of seasonal variations in temperature.

4.3. Limitations

In this study, we considered the impact of slow temperature acclimation of photosynthesis on GPP estimation and established T_a and S models to simulate GPP, respectively. The results showed that considering the slow temperature acclimation could improve the accuracy of GPP estimation. We also used CSIF and T_a derived from ERA-5 to map the global spatial distribution of the time constant- τ which exhibited significant spatial patterns. Nevertheless, there are still some limitations in this study. Firstly, we didn't consider the seasonal and interannual variations of τ values when we established models. In theory, the temperature acclimation capacity of vegetation differs in different growth stages, that is, the τ values exist seasonal or interannual variations (Chen and Zhuang 2013; Crous et al. 2022; Kolari et al. 2014; Kumarathunge et al. 2019; Trewavas 2009; Zhang et al. 2023a; Zhang et al. 2023b). In this study, we set the τ values as a constant through all seasons and ignored its variations. In the future, we should incorporate the seasonal variations of τ values into S calculation which may get the higher improvement in GPP quantification. Secondly, at the site scale, in order to ensure high temporal resolution (1 day), SW was used to characterize radiation, so variables representing the growth state of vegetation are not considered (e.g., Absorbed Photosynthetically Active Radiation (APAR)). The reason why we didn't use APAR in each site is that APAR is usually calculated through FPAR (Fraction of Photosynthetically Active Radiation) derived from satellite remote sensing which always has a temporal resolution greater than 4 days and is not consistent with the daily flux site datasets. The only difference between the explanatory variables of T_a and S models was S and T_a. Therefore, the difference between the GPP estimation based on these two models was mostly induced by the considering the slow temperature acclimation or not. To confirm this point, we chose a flux site (US-NR1) and replaced the explanatory variable-SW in both models with APAR and tested the performance of T_a and S models with APAR as the explanatory variable. Since the temporal resolution of FPAR is 8 days, to ensure the amount of data used for model establishment and validation, we assigned FPAR data every 8 days to daily site data and assumed that there is no change in FPAR within 8 days. Fig. S3 and Fig. S4 showed the validation results of SW and APAR as explanatory variables in both T_a and S models, respectively, with 1-day temporal resolution at US-NR1. In addition, the APAR with 8-day temporal resolution and the corresponding SW as explanatory variables of both T_a and S models, respectively, were also built and validated at US-NR1 (Fig. S5, Fig. S6). The results showed that S model still performed better than T_a model when SW was replaced with APAR at both daily and 8-day temporal resolution (see Fig. S3-Fig. S6). Thirdly, we used the machine learning method (random forest algorithm) to simulate GPP. We cannot understand the internal structure of the machine learning models although they always have good simulation performance. The reason why we used RF to simulate GPP was that the initial goal of this study was to explore whether considering the slow temperature acclimation of photosynthesis could improve the accuracy of GPP estimates. And the results indeed confirmed that the accuracy of GPP simulation was improved when we considered the slow temperature acclimation. In the future, we should try to embed S into some process-based or semi-empirical models, e.g., LUE models, which will provide more accurate GPP quantification. Moreover, the temporal resolution of CSIF dataset (4-day) is insufficient to map more detailed global spatial distribution of τ values especially in the regions with lower τ values. For example, in the high latitude regions

of the northern hemisphere where vegetation is highly sensitive to temperature, the 4-day temporal resolution may still be too coarse to capture more accurate τ values. If a new SIF dataset with higher temporal resolution appears in the future, this issue will be improved to some extent. Last, we did not account for the impact of other environmental factors affecting the temperature response of photosynthesis, such as, VPD, precipitation, radiation, soil moisture and so on (Lin et al. 2012), which need further investigation in the future.

5. Conclusion

In this study, we established T_a and S models based on RF, respectively, to analyze the influence of slow temperature acclimation of photosynthesis on GPP estimation. We also mapped the global spatial distribution of the time it takes for vegetation to acclimate temperature. We obtained the following conclusions:

(1) Considering the slow temperature acclimation could improve the accuracy of GPP estimation. Compared to T_a model, the R^2 value of S model increased from 0.62 to 0.74 which was increased 19.35%; the RMSE value of S model reduced from 2.59 to 2.17 g $C/m^2/d$ which was reduced 16.21%; and the slope value of S model increased from 0.69 to 0.78 which was increased 13.04%.
(2) The improvement of S model in GPP estimations was different in different vegetation growth stages which was larger in the springtime recovery of photosynthesis than that in the rapid growing and autumn decline stages.
(3) Both T_a and S could characterize the overall seasonal trends of GPP well. However, considering the slow temperature acclimation can reduce the sensitivity of vegetation to temperature and avoid the excessive fluctuations in GPP estimation induced by temperature changes.
(4) The τ values showed significant spatial distribution. The lower τ values mainly appeared in boreal and temperate areas, and the higher τ values mainly existed in some both warmer and arid areas, which was strongly affected by the growth strategies determined by the limiting factors of vegetation growth and seasonal variations in temperature.

CRediT authorship contribution statement

Jia Bai: Writing – review & editing, Writing – original draft, Visualization, Validation, Software, Resources, Methodology, Investigation, Formal analysis, Data curation, Conceptualization. **Helin Zhang:** Writing – review & editing, Visualization, Software, Investigation, Formal analysis. **Rui Sun:** Writing – review & editing, Supervision, Resources, Project administration, Investigation, Funding acquisition, Conceptualization. **Yuhao Pan:** Writing – review & editing, Validation, Software, Formal analysis.

Declaration of competing interest

The authors declare no conflict of interest.

Data availability

Data will be made available on request.

Acknowledgments

This work was supported by the National Natural Science Foundation of China (42271330). We thank to the hard work of Dr. Yao Zhang, et al. for producing the CSIF and sharing this dataset. This work also used the eddy covariance data acquired by the FLUXNET2015, we sincerely thank all FLUXNET2015 communities of the eddy covariance data https://fluxnet.fluxdata.org/data/. We thank the anonymous reviewers for their helpful suggestions on the manuscript.

Supplementary materials

Supplementary material associated with this article can be found, in the online version, at doi:10.1016/j.agrformet.2024.110197.

References

Anav, A., Friedlingstein, P., Beer, C., et al., 2015. Spatiotemporal patterns of terrestrial gross primary production: a review. Rev. Geophys. 53, 785–818.
Aspinwall, M.J., Drake, J.E., Campany, C., et al., 2016. Convergent acclimation of leaf photosynthesis and respiration to prevailing ambient temperatures under current and warmer climates in Eucalyptus tereticornis. New Phytol. 212, 354–367.
Atkin, O.K., Atkinson, L.J., Fisher, R.A., et al., 2008. Using temperature-dependent changes in leaf scaling relationships to quantitatively account for thermal acclimation of respiration in a coupled global climate–vegetation model. Glob. Change Biol. 14, 2709–2726.
Badgley, G., Anderegg, L.D.L., Berry, J.A., et al., 2019. Terrestrial gross primary production: using NIRV to scale from site to globe. Glob. Change Biol. 25, 3731–3740.
Baldocchi, D., 2014. Measuring fluxes of trace gases and energy between ecosystems and the atmosphere – the state and future of the eddy covariance method. Glob. Change Biol. 20, 3600–3609.
Baldocchi, D.D., 2003. Assessing the eddy covariance technique for evaluating carbon dioxide exchange rates of ecosystems: past, present and future. Glob. Change Biol. 9, 479–492.
Battin, T.J., Luyssaert, S., Kaplan, L.A., et al., 2009. The boundless carbon cycle. Nat. Geosci. 2, 598–600.
Beer, C., Reichstein, M., Tomelleri, E., et al., 2010. Terrestrial gross carbon dioxide uptake: global distribution and covariation with climate. Science (1979) 329, 834–838.
Berry, J., Bjorkman, O., 1980. Photosynthetic response and adaptation to temperature in higher plants. Annu Rev. Plant Physiol. 31, 491–543.
Carter, K.R., Wood, T.E., Reed, S.C., et al., 2020. Photosynthetic and respiratory acclimation of understory shrubs in response to *in situ* experimental warming of a wet tropical forest. Front. For. Glob. Change 3.
Chen, A., Mao, J., Ricciuto, D., et al., 2021a. Seasonal changes in GPP/SIF ratios and their climatic determinants across the Northern hemisphere. Glob. Change Biol. *n/a*.
Chen, A., Mao, J., Ricciuto, D., et al., 2021b. Moisture availability mediates the relationship between terrestrial gross primary production and solar-induced chlorophyll fluorescence: insights from global-scale variations. Glob. Change Biol. 27, 1144–1156.
Chen, J.M., Liu, J., Cihlar, J., et al., 1999. Daily canopy photosynthesis model through temporal and spatial scaling for remote sensing applications. Ecol. Modell. 124, 99–119.
Chen, M., Zhuang, Q., 2013. Modelling temperature acclimation effects on the carbon dynamics of forest ecosystems in the conterminous United States. Tellus B Chem. Phys. Meteorol.
Cheng, Y.-B., Zhang, Q., Lyapustin, A.I., et al., 2014. Impacts of light use efficiency and fPAR parameterization on gross primary production modeling. Agric. For. Meteorol. 189-190, 187–197.
Crous, K.Y., Uddling, J., De Kauwe, M.G., 2022. Temperature responses of photosynthesis and respiration in evergreen trees from boreal to tropical latitudes. New Phytol. 234, 353–374.
Cunningham, S., Read, J., 2003a. Comparison of temperate and tropical rainforest tree species: growth responses to temperature. J. Biogeogr. 30, 143–153.
Cunningham, S.C., Read, J., 2003b. Do temperate rainforest trees have a greater ability to acclimate to changing temperatures than tropical rainforest trees? New Phytol. 157, 55–64.
Dusenge, M.E., Duarte, A.G., Way, D.A., 2019. Plant carbon metabolism and climate change: elevated CO2 and temperature impacts on photosynthesis, photorespiration and respiration. New Phytol. 221, 32–49.
Dusenge, M.E., Madhavji, S., Way, D.A., 2020. Contrasting acclimation responses to elevated CO2 and warming between an evergreen and a deciduous boreal conifer. Glob. Change Biol. 26, 3639–3657.
Fang, L., Martre, P., Jin, K., et al., 2023. Neglecting acclimation of photosynthesis under drought can cause significant errors in predicting leaf photosynthesis in wheat. Glob. Change Biol. 29, 505–521.
Frankenberg, C., Berry, J., Liang, S., 2018. 3.10 - Solar induced chlorophyll fluorescence: origins, relation to photosynthesis and retrieval. Comprehensive Remote Sensing. Elsevier, Oxford, pp. 143–162.
Frankenberg, C., Fisher, J.B., Worden, J., et al., 2011. New global observations of the terrestrial carbon cycle from GOSAT: patterns of plant fluorescence with gross primary productivity. Geophys. Res. Lett. 38.
Frankenberg, C., O'Dell, C., Berry, J., et al., 2014. Prospects for chlorophyll fluorescence remote sensing from the Orbiting Carbon Observatory-2. Remote Sens. Environ. 147, 1–12.
Gea-Izquierdo, G., Mäkelä, A., Margolis, H., et al., 2010. Modeling acclimation of photosynthesis to temperature in evergreen conifer forests. New Phytol. 188, 175–186.

Guan, X., Chen, J.M., Shen, H., et al., 2021. A modified two-leaf light use efficiency model for improving the simulation of GPP using a radiation scalar. Agric. For. Meteorol. 307, 108546.
Guanter, L., Alonso, L., Gómez-Chova, L., et al., 2007. Estimation of solar-induced vegetation fluorescence from space measurements. Geophys. Res. Lett. 34.
Guanter, L., Frankenberg, C., Dudhia, A., et al., 2012. Retrieval and global assessment of terrestrial chlorophyll fluorescence from GOSAT space measurements. Remote Sens. Environ. 121, 236–251.
Guo, M., Li, J., Huang, S., et al., 2020. Feasibility of using MODIS products to simulate sun-induced chlorophyll fluorescence (SIF) in boreal forests. Remote Sens. 12 (Basel).
Guo, Y., Li, G., Chen, H., et al., 2017. An enhanced PCA method with savitzky-golay method for VRF system sensor fault detection and diagnosis. Energy Build. 142, 167–178.
He, M., Ju, W., Zhou, Y., et al., 2013. Development of a two-leaf light use efficiency model for improving the calculation of terrestrial gross primary productivity. Agric. For. Meteorol. 173, 28–39.
Hember, R.A., Kurz, W.A., Coops, N.C., 2017. Increasing net ecosystem biomass production of Canada's boreal and temperate forests despite decline in dry climates. Global. Biogeochem. Cycles 31, 134–158.
Hikosaka, K., Ishikawa, K., Borjigidai, A., et al., 2006. Temperature acclimation of photosynthesis: mechanisms involved in the changes in temperature dependence of photosynthetic rate. J. Exp. Bot. 57, 291–302.
Hu, J., Liu, L., Yu, H., et al., 2021. Upscaling GOME-2 SIF from clear-sky instantaneous observations to all-sky sums leading to an improved SIF–GPP correlation. Agric. For. Meteorol. 306, 108439.
Janssens, I.A., Freibauer, A., Ciais, P., et al., 2003. Europe's terrestrial biosphere absorbs 7 to 12% of European anthropogenic CO2 emissions. Science 300, 1538–1542 (1979).
Jiang, C., Ryu, Y., 2016. Multi-scale evaluation of global gross primary productivity and evapotranspiration products derived from Breathing Earth System Simulator (BESS). Remote Sens. Environ. 186, 528–547.
Jung, M., Reichstein, M., Margolis, H.A., et al., 2011. Global patterns of land-atmosphere fluxes of carbon dioxide, latent heat, and sensible heat derived from eddy covariance, satellite, and meteorological observations. J. Geophys. Res. Biogeosci. 116.
Karban, R., 2008. Plant behaviour and communication. Ecol. Lett. 11, 727–739.
Köehler, P., Frankenberg, C., Magney, T.S., et al., 2018. Global retrievals of solar-induced chlorophyll fluorescence with TROPOMI: first results and intersensor comparison to OCO-2. Geophys. Res. Lett. 45.
Köhler, P., Guanter, L., Kobayashi, H., et al., 2018. Assessing the potential of sun-induced fluorescence and the canopy scattering coefficient to track large-scale vegetation dynamics in Amazon forests. Remote Sens. Environ. 204, 769–785.
Kolari, P., Chan, T., Porcar-Castell, A., et al., 2014. Field and controlled environment measurements show strong seasonal acclimation in photosynthesis and respiration potential in boreal Scots pine. Front. Plant Sci. 5.
Kolari, P., Kulmala, L., Pumpanen, J., et al., 2009. CO2 exchange and component CO2 fluxes of a boreal scots pine forest. Boreal Environ. Res. 14, 761–783.
Kolari, P., Lappalainen, H.K., HÄNninen, H., et al., 2007. Relationship between temperature and the seasonal course of photosynthesis in Scots pine at northern timberline and in southern boreal zone. Tellus B 59, 542–552.
Krämer, J., Siegmann, B., Kraska, T., et al., 2021. The potential of spatial aggregation to extract remotely sensed sun-induced fluorescence (SIF) of small-sized experimental plots for applications in crop phenotyping. Int. J. Appl. Earth Obs. Geoinf. 104, 102565.
Kumarathunge, D.P., Medlyn, B.E., Drake, J.E., et al., 2019. Acclimation and adaptation components of the temperature dependence of plant photosynthesis at the global scale. New Phytol. 222, 768–784.
Leuendorf, J.E., Frank, M., Schmülling, T., 2020. Acclimation, priming and memory in the response of Arabidopsis thaliana seedlings to cold stress. Sci. Rep. 10, 689.
Lin, Y.-S., Medlyn, B.E., Ellsworth, D.S., 2012. Temperature responses of leaf net photosynthesis: the role of component processes. Tree Physiol. 32, 219–231.
Lombardozzi, D.L., Bonan, G.B., Smith, N.G., et al., 2015. Temperature acclimation of photosynthesis and respiration: a key uncertainty in the carbon cycle-climate feedback. Geophys. Res. Lett. 42, 8624–8631.
Luo, X., Keenan, T.F., 2020. Global evidence for the acclimation of ecosystem photosynthesis to light. Nat. Ecol. Evol. 4, 1351–1357.
Ma, J., Yan, X., Dong, W., et al., 2015. Gross primary production of global forest ecosystems has been overestimated. Sci. Rep. 5, 10820.
Mäkelä, A., Hari, P., Berninger, F., et al., 2004. Acclimation of photosynthetic capacity in Scots pine to the annual cycle of temperature. Tree Physiol. 24, 369–376.
MÄKelÄ, A., Pulkkinen, M., Kolari, P., et al., 2008. Developing an empirical model of stand GPP with the LUE approach: analysis of eddy covariance data at five contrasting conifer sites in Europe. Glob. Change Biol. 14, 92–108.
Mkel, A., Givnish, T.J., Berninger, F., et al., 2002. Challenges and opportunities of the optimality approach in plant ecology. Silva Fennica 36, 605–614.
Mohammed, G.H., Colombo, R., Middleton, E.M., et al., 2019. Remote sensing of solar-induced chlorophyll fluorescence (SIF) in vegetation: 50 years of progress. Remote Sens. Environ. 231, 111177.
Pastorello, G., Trotta, C., Canfora, E., et al., 2020. The FLUXNET2015 dataset and the ONEFlux processing pipeline for eddy covariance data. Sci. Data 7, 225.
Piao, S., Liu, Q., Chen, A., et al., 2019. Plant phenology and global climate change: current progresses and challenges. Glob. Change Biol. 25, 1922–1940.
Piao, S., Wang, X., Wang, K., et al., 2020. Interannual variation of terrestrial carbon cycle: issues and perspectives. Glob. Change Biol. 26, 300–318.
Porcar-Castell, A., Malenovský, Z., Magney, T., et al., 2021. Chlorophyll a fluorescence illuminates a path connecting plant molecular biology to Earth-system science. Nat. Plants 7, 998–1009.
Porcar-Castell, A., Tyystjärvi, E., Atherton, J., et al., 2014. Linking chlorophyll a fluorescence to photosynthesis for remote sensing applications: mechanisms and challenges. J. Exp. Bot. 65, 4065–4095.
Potter, C.S., Randerson, J.T., Field, C.B., et al., 1993. Terrestrial ecosystem production: a process model based on global satellite and surface data. Global. Biogeochem. Cycles 7, 811–841.
Preston, J., Sandve, S., 2013. Adaptation to seasonality and the winter freeze. Front. Plant Sci. 4.
Reich, P.B., Sendall, K.M., Stefanski, A., et al., 2018. Effects of climate warming on photosynthesis in boreal tree species depend on soil moisture. Nature 562, 263–267.
Running, S.W., Nemani, R.R., Heinsch, F.A., et al., 2004. A continuous satellite-derived measure of global terrestrial primary production. Bioscience 54, 547–560.
Sabot, M.E.B., De Kauwe, M.G., Pitman, A.J., et al., 2022. Predicting resilience through the lens of competing adjustments to vegetation function. Plant Cell Environ. 45, 2744–2761.
Smith, N.G., Dukes, J.S., 2013. Plant respiration and photosynthesis in global-scale models: incorporating acclimation to temperature and CO2. Glob. Change Biol. 19, 45–63.
Smith, N.G., Dukes, J.S., 2017. Short-term acclimation to warmer temperatures accelerates leaf carbon exchange processes across plant types. Glob. Change Biol. 23, 4840–4853.
Smith, N.G., Malyshev, S.L., Shevliakova, E., et al., 2016. Foliar temperature acclimation reduces simulated carbon sensitivity to climate. Nat. Clim. Change 6, 407–411.
Sun, Y., Frankenberg, C., Jung, M., et al., 2018. Overview of solar-induced chlorophyll fluorescence (SIF) from the orbiting carbon observatory-2: retrieval, cross-mission comparison, and global monitoring for GPP. Remote Sens. Environ. 209, 808–823.
Trewavas, A., 2009. What is plant behaviour?*. Plant Cell Environ. 32, 606–616.
Valladares, F., Matesanz, S., Guilhaumon, F., et al., 2014. The effects of phenotypic plasticity and local adaptation on forecasts of species range shifts under climate change. Ecol. Lett. 17, 1351–1364.
Wang, S., Huang, K., Yan, H., et al., 2015. Improving the light use efficiency model for simulating terrestrial vegetation gross primary production by the inclusion of diffuse radiation across ecosystems in China. Ecol. Complex. 23, 1–13.
Wu, D., Zhao, X., Liang, S., et al., 2015. Time-lag effects of global vegetation responses to climate change. Glob. Change Biol. 21, 3520–3531.
Xiao, J., Chevallier, F., Gomez, C., et al., 2019. Remote sensing of the terrestrial carbon cycle: a review of advances over 50 years. Remote Sens. Environ. 233, 111383.
Yu, L., Wen, J., Chang, C.Y., et al., 2019. High-Resolution Global Contiguous SIF of OCO-2. Geophys. Res. Lett. 46, 1449–1458.
Zarco-Tejada, P.J., Pushnik, J.C., Dobrowski, S., et al., 2003. Steady-state chlorophyll a fluorescence detection from canopy derivative reflectance and double-peak red-edge effects. Remote Sens. Environ. 84, 283–294.
Zhang, H., Bai, J., Sun, R., et al., 2023a. Improved global gross primary productivity estimation by considering canopy nitrogen concentrations and multiple environmental factors. Remote Sens. 15, 698 (Basel).
Zhang, H., Bai, J., Sun, R., et al., 2023b. An improved light use efficiency model by considering canopy nitrogen concentrations and multiple environmental factors. Agric. For. Meteorol. 332, 109359.
Zhang, M., Yu, G.-R., Zhuang, J., et al., 2011. Effects of cloudiness change on net ecosystem exchange, light use efficiency, and water use efficiency in typical ecosystems of China. Agric. For. Meteorol. 151, 803–816.
Zhang, Q., Chen, J.M., Ju, W., et al., 2021. Ground-based multiangle solar-induced chlorophyll fluorescence observation and angular normalization for assessing crop productivity. J. Geophys. Res. Biogeosciences 126, e2020JG006082.
Zhang, X., Friedl, M.A., Schaaf, C.B., et al., 2003. Monitoring vegetation phenology using MODIS. Remote Sens. Environ. 84, 471–475.
Zhang, Y., Joiner, J., Alemohammad, S.H., et al., 2018. A global spatially contiguous solar-induced fluorescence (CSIF) dataset using neural networks. Biogeosciences. 15, 5779–5800.
Zhang, Y., Piao, S., Sun, Y., et al., 2022. Future reversal of warming-enhanced vegetation productivity in the Northern Hemisphere. Nat. Clim. Change 12, 581–586.
Zhang, Y., Xiao, X., Jin, C., et al., 2016. Consistency between sun-induced chlorophyll fluorescence and gross primary production of vegetation in North America. Remote Sens. Environ. 183, 154–169.
Zhang, Z., Chen, J.M., Guanter, L., et al., 2019. From canopy-leaving to total canopy far-red fluorescence emission for remote sensing of photosynthesis: first results from TROPOMI. Geophys. Res. Lett. 46, 12030–12040.
Zheng, Y., Shen, R., Wang, Y., et al., 2020. Improved estimate of global gross primary production for reproducing its long-term variation, 1982–2017. Earth Syst. Sci. Data 12, 2725–2746.
Zhou, L., Tucker, C.J., Kaufmann, R.K., et al., 2001. Variations in northern vegetation activity inferred from satellite data of vegetation index during 1981 to 1999. J. Geophys. Res. Atmos. 106, 20069–20083.
Zuther, E., Juszczak, I., Ping Lee, Y., et al., 2015. Time-dependent deacclimation after cold acclimation in Arabidopsis thaliana accessions. Sci. Rep. 5, 12199.